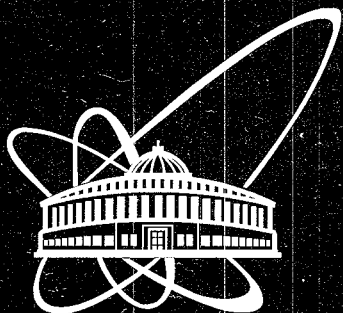




XJ0100127



**ОБЪЕДИНЕННЫЙ
ИНСТИТУТ
ЯДЕРНЫХ
ИССЛЕДОВАНИЙ**

Дубна

E10-2001-48

N.D.Dikoussar*

**A LOCAL CUBIC SMOOTHING
IN AN ADAPTATION MODE**

Submitted to «Computer Physics Communications»

*E-mail: dikoussar@vxjinr.jinr.ru

2001

1. Introduction

The curve smoothing (approximation) is the fundamental problem in mathematics, practical statistics and data analysis. The development of effective methods and algorithms of smoothing is an issue of modern technologies. The efficiency of the algorithm includes such main properties, as simplicity of calculations, stability to noises and backgrounds, accuracy of a curve estimation, adaptability of algorithm.

Non-parametric linear regression methods have been developed intensively in recent decades. The well-known techniques such as kernel smoothing, nearest neighbor smoothing, spline smoothing, local regression and wavelet analysis [1,2,8] are widely used in data analysis. The curve smoothing is used in several applications areas [3-7], such as digital signal processing, track finding, image processing, system identification and so on. Data analysis in such systems is usually carried out in a real-time mode. Classical methods, such as the high orders recursive least squares method (RLSM) or kalman estimation [3] are poorly suitable due to their computing complexity and instability.

The proposed method is based on a new approach to smoothing the curve, named as the 4-point transforms or DPT (discrete projective transforms) [9]. A simple iterative procedure for estimation of a parameter of a three-point cubic model (TPS) has been derived using DPT and the first order RLSM. A rate of convergence of iterations is controlled by parameters and a process in itself is similar to the Robbins-Monroe procedure known in stochastic approximation [10]. A smoother using this method is stable to random errors and very simple in computing. It obtains fitted values in an adaptive mode and can work in the data inflow regime. The curve segment is estimated as a continuous cubic curve.

In the proposed approach the relationship between points (samples) is determined by weight functions, equal to cross-ratio (CR) functions of four points $\{0, \lambda, L, \tau\}$, located on the real axis x [9]. There are two kinds of CR-functions: $\{p_i = p_i(\tau; \lambda, L)\}$ and $\{d_i = d_i(\tau; \lambda, L)\}$, $i=1,2,3$. The functions $\{p_i\}$ are used as effective noise-suppressing tools for simplification of the curve shape. Functions $\{d_i\}$ and cubic monospline $Q(\tau; \lambda, L)$ are used as building units of the curve. 3D vectors $\mathbf{Y}^T = [y_\lambda, y_L, y_\tau]$ (observation) and $\mathbf{P}^T = [p_1, p_2, p_3]$, $\mathbf{D}^T = [d_1, d_2, d_3]$ (weight vectors) are used for operations with an arbitrary point of the curve y_τ .

A three point cubic spline [9,11] is taken as a basic model of the curve (TPS-model). Main parameters of the TPS-model are: three fixed points on the curve presented as vector $\mathbf{R}_0^T = [\tilde{R}_\lambda, \tilde{R}_L, \tilde{R}_0]$, one free parameter θ , a number of samples n_θ and boundary knots x_b, x_e of the interval, for which the cubic model shapes the curve within a given threshold of accuracy. An arbitrary ordinate of the cubic curve is obtained by summation of a "fixed quadratic parabola" $\Pi[\tau; \lambda, L; \mathbf{R}_0] = (\mathbf{R}_0, \mathbf{D})$ and a cubic parabola $\theta Q(\tau; \lambda, L)$, where θ is a free parameter.

For $\sigma_e^2 < \infty$ estimates $\hat{\theta}$ and $\hat{\mathbf{R}}_0$ are determined in two stages. First, the estimate $\hat{\theta}$, n_θ and x_b, x_e are calculated in a recurrent way using $\hat{\mathbf{R}}_0$ and then $\hat{\mathbf{R}}_0$ is found using output of the first stage and the simple least squares method (LSM).

The TPS-model differs from the standard cubic model in which all four parameters are free. The parameters \mathbf{R}_0 allow easily to be fixed on a curve using its three points whereas the shape of the curve can be determined by variation of the free parameter. In addition, abscisses of the fixed points are used as parameters of weight functions that give such a construction a property of self-consistency.

This paper presents new methods and algorithms for a local cubic curve approximation and the smoothing, using DPT and TPS-model. A new effective recursive procedure and the algorithm of the local cubic smoother (LOCUS) are developed.

An efficiency of the LOCUS is proved by mathematical tools and by examples of using this algorithm for a piecewise cubic approximation, and the smoothing of an arbitrary function $\tilde{f}(x) = f(x) + e(x)$, $f(x) \in C$, $x \in [a, b]$, given by a set of consecutive points (samples) $\{x_k, \tilde{y}_k\}$, $k = 1, 2, \dots, N$, ($N \gg 4$), where $e(x) \sim N(0, \sigma_e^2)$ for definiteness. An estimate of the function is given as a sum of M local cubic splines $S_j(x; \hat{\Theta})$ ($I(x)$ is an indicator function) in the following form

$$\hat{f}(x) \approx \sum_{j=1}^M I_j(x) S_j(x; \hat{\Theta}_j), \quad I_j(x) = \begin{cases} 1, & x \in [x_{b_j}, x_{e_j}] \\ 0, & x \notin [x_{b_j}, x_{e_j}] \end{cases}, \quad [x_{b_j}, x_{e_j}] \subseteq [a, b], \quad M \geq 1, \quad (1)$$

provided the smoothing (approximation) error does not exceed a given threshold of accuracy T_f

$$\max_{x \in [x_{b_j}, x_{e_j}]} |\tilde{f} - S_j| < T_f, \quad (2)$$

where x_{b_j} and x_{e_j} are left and right knots and $\hat{\Theta}_j$ is mean-square estimates of \mathbf{R}_0 and θ for S_j . The knots are determined automatically using the criterion (2).

As we know, an optimum choice of knots in representation of $f(x)$ by a global spline is the difficult problem [12]. In use of LSM, a choice of knots for estimation of an approximating polynomial is determined, as a rule, by a trial and error method.

LOCUS can be used for a tabulated curve as a tool for recovering some features or parameters from values $\{\tilde{f}_k\}$ and as data compression as well. If $f(x)$ is defined by a formula, then practical use of LOCUS has interest from the computing point of view, for example, in searching a local extreme, or initial values of roots. Mention must be made that solving task (1)-(2) by LOCUS has a very simple computing circuit and uses a small size of memory as compared with the traditional linear regression algorithms.

Section 2 gives the basic conception of the 4-point transforms, the TPS-model and demonstrates a stability of DPT to random errors. Section 3 describes the recursive procedure of the cubic smoother based on DPT and the first order RLSP. A passage to computation on parameters and algorithm LOCUS is described in Section 4. Sections 5 and 6 contains examples of the curve smoothing and results of comparison of LOCUS with other smoothers.

2. The 4-point transforms and the cubic model

This section considers the main properties of the 4-point transforms and construction of the TPS-model.

2.1. DPT or 4-point transforms

Let points $\{(x_k, \tilde{f}_k)\}$, $k = 1, 2, \dots, K_{\max}$ be arranged in series on the noise curve $\tilde{f}_k = f(x_k) + e_k$, $x_k \in [a, b]$, $e(x) \sim N(0, \sigma_e^2)$, where $f(x) \in C$, $x \in [a, b]$.

Let us take three non-coinciding points $x_{k_0}, x_{k_\lambda}, x_{k_L} \in \{x_k\}$ and fix on the curve three points as a mark $\mathfrak{R} : \{(x_{k_0}, \tilde{R}_0); (x_{k_\lambda}, \tilde{R}_\lambda); (x_{k_L}, \tilde{R}_L)\}$, $\tilde{R}_0, \tilde{R}_\lambda, \tilde{R}_L \in \{\tilde{f}_k\}$.

Using $x_{k_0}, x_{k_\lambda}, x_{k_L}$ one can define three parameters: $x_0 \equiv x_{k_0}$ (the basic point) and two pole points $\lambda = x_{k_\lambda} - x_{k_0}$ and $L = x_{k_L} - x_{k_0}$. For simplification we shall transfer the origin at the basic point

$$\tau_k = x_k - x_0, \quad \tilde{\phi}_k = \tilde{f}_k - \tilde{R}_0$$

and denote three fixed parameters of the curve as follows

$$\tilde{\theta}_{x_0} \equiv \tilde{R}_0; \quad \tilde{\theta}_\lambda \equiv \tilde{\phi}_\lambda = \tilde{R}_\lambda - \tilde{R}_0; \quad \tilde{\theta}_L \equiv \tilde{\phi}_L = \tilde{R}_L - \tilde{R}_0.$$

Using the fixed parameters and $\{\tilde{f}_k\}$, we can form the observation vectors as

$$\tilde{\mathbf{Y}}_k^T = [\tilde{\theta}_\lambda, \tilde{\theta}_L, \tilde{\phi}_k], \quad k = 1, 2, \dots, K_{\max}.$$

Following [9], let us compute weight vectors at the point τ_k

$$\mathbf{P}_k^T = [p_{1k}, p_{2k}, p_{3k}], \quad (k \neq k_\lambda \neq k_L) \text{ and } \mathbf{D}_k^T = [d_{1k}, d_{2k}, d_{3k}],$$

where the functions $p_{ik} = p_i(\tau_k; \lambda, L)$ and $d_{ik} = d_i(\tau_k; \lambda, L)$ are defined by means of a cross-ratio $\frac{13}{24} : \frac{23}{14}$ of four points $\{0, \lambda, L, \tau_k\}$, $k = 1, 2, \dots, K_{\max}$, $i = 1, 2, 3$ (Fig. 1). In what follows we shall use *CRw* as the abbreviation for the "cross-ratio weights".

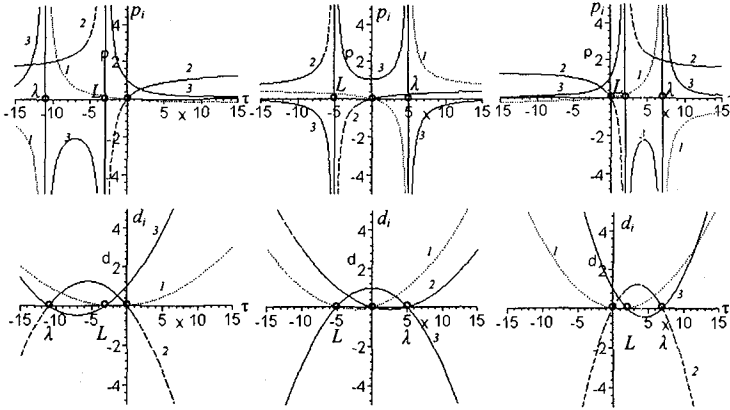


Fig. 1. Shapes of *CRw* functions for various values of λ and L .

Then the direct 4-point transform of $\tilde{\phi}(\tau)$ at point τ_k , ($k = 1, 2, \dots, K_{\max}$, $k \neq k_\lambda \neq k_L$) for given \mathfrak{R} is defined as three-point convolution of the observation vector $\tilde{\mathbf{Y}}_k$ with the weight vector \mathbf{P}_k [9]

$$\tilde{\phi}_k^{\triangleleft} \equiv \tilde{\phi}^{\triangleleft}(\tau_k; \mathfrak{R}) = (\tilde{\mathbf{Y}}_k, \mathbf{P}_k). \quad (3)$$

The inverse 4-point transformation is defined as

$$[\tilde{\phi}_k^{\leftarrow}]^{\text{P}} \equiv \tilde{\phi}(\tau_k; \mathfrak{R}) = (\mathbf{Z}_k, \mathbf{D}_k), \quad (4)$$

where $\tilde{\mathbf{Z}}_k^T = [\tilde{\theta}_\lambda, \tilde{\theta}_L, \tilde{\phi}_k^{\leftarrow}]$, $k = 1, 2, \dots, K_{\max}$.

The calculations of p_{ik} at τ_k are carried out in accordance with above cross-ratio of four points $\{0, \tau_k, \lambda, L\}$. One can see that CRw-functions make up a *system of functions with threefold symmetry*. The properties of such functions is given in [9, 13]. To obtaining CRw at τ_k we use the basic "generating" function p_3 :

$$p_3(\tau_k; \lambda, L) = \frac{\lambda L}{(\tau_k - \lambda)(\tau_k - L)}, \lambda \neq L \neq \tau_k, \lambda, L \neq 0. \quad (5)$$

Using (5) one can easily to calculate all other weight functions. So, p_{1k} and p_{2k} are obtained by means of rearrangements $\lambda \leftrightarrow \tau_k$ and $L \leftrightarrow \tau_k$ in p_{3k} respectively. In view of $p_{3k} \neq 0$ and $\sum_i p_{ik} = 1$, the functions d_{ik} can be expressed through p_{ik} as

$$d_{ik} = (-p_{ik})^j / p_{3k}, \quad j = (3i - i^2) / 2, \quad \sum_i d_{ik} = 1, \quad i = 1, 2, 3. \quad (5a)$$

If $f(x)$ is assigned with a step of grid h , then CRw depend only from indices k owing to scale invariance of Eq. (5), i.e.

$$p_{ik} = p_i(k; k_\lambda, k_L), \quad d_{ik} = d_i(k; k_\lambda, k_L), \quad k_\lambda \neq k_L.$$

In what follows, values $k_\lambda = \lambda / h$ and $k_L = L / h$ are labeled as μ and m pro tanto.

2.2. The TPS-model

In ref. [9] the formula for approximation of $f(x) \subset C$, $x \in [a, b]$ was offered as the sum of the square-law parabola $\Pi(\tau; \mathfrak{R})$ fixed by the mark \mathfrak{R} and by the set of N_α , ($N_\alpha \geq 3$) monosplines $S_k(\tau; \lambda, L)$ of the k -th order ensuring a uniform approximation of $f(x)$ on the segment $[x_\lambda, x_L]$:

$$f(x) \approx \Pi(\tau; \mathfrak{R}) + \sum_{k=3}^{N_\alpha} \alpha_k(\lambda, L) S_k(\tau; \lambda, L), \quad (6)$$

where $\alpha_k(\lambda, L)$ is unknown parameters, and $\tau = x - x_0$.

From (6) at $N_\alpha = 3$ we obtain the model of the local three-point cubic spline (TPS) as

$$S(\tau; \Theta) = S_3(\tau; \mathfrak{R}) = (\mathbf{R}_0, \mathbf{D}) + \theta Q(\tau; \lambda, L), \quad (7)$$

where Θ denotes a set of parameters \mathbf{R}_0 and θ . θ is the unknown free parameter, $Q(\tau; \lambda, L) = \tau(\tau - \lambda)(\tau - L)$ - the "zeroed" cubic parabola, $\mathbf{R}_0^T = [R_\lambda, R_L, R_0]$ - the vector of the pivot ordinates. In terms of the vectors \mathbf{R}_0 and \mathbf{D} , the equation of "the pivot parabola" looks as $\Pi(\tau; \mathfrak{R}) = (\mathbf{R}_0, \mathbf{D})$ (Fig. 2). For the given \mathfrak{R} the model (7) depends only upon the unknown parameter θ . Fig. 3 shows changing the shapes of the cubic curves (7), depending upon choice of θ_m , $m = 1, \dots, 7$ for fixed λ, L and \mathbf{R}_0 . When $f(x)$ is defined by formula, then θ is determined exactly [9]:

$$\theta = \frac{1}{H^2} [f'(x_\lambda) + f'(x_L) - \frac{2}{H} (R_L - R_\lambda)], \quad H = L - \lambda. \quad (8)$$

Thus, it follows from Eqs. (7) and (8) that using the TPS-model for the cubic approximation of $f(x), x \in [x_\lambda, x_L]$ we only use a first derivative of the function at points x_λ and x_L and the coordinates of three points (for comparison: Taylor formula uses one point and *three* values of derivatives at the point x_0). In this case we emphasize that the TPS-model provides a *uniformed* character of the approximation error on the segment $[x_\lambda, x_L]$ at $x_\lambda < x_0 < x_L$.

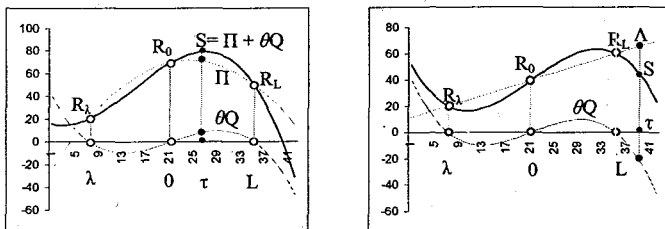


Fig. 2. The TPS-model.

This property of the TPS-model is very useful in smoothing a noise tabulated function given at a discrete grid. As it was noted in [9] the LSM - estimation of the parameter θ in smoothing a cubic curve by the TPS-model has the following simple form:

$$\hat{\theta} = (\lambda L \sum_{k=1}^n \tau_k^2)^{-1} \sum_{k=1}^n \tau_k \tilde{\phi}_k^a, \quad (9)$$

where notation $\tilde{\phi}_k^a$ sets the 4-point transform of function $\tilde{\phi}_k$ at the point τ_k (Eq.3). To avoid a "gross error" of the transformed value, the point τ_k should be taken out of the "noisy zones" defined by the threshold T_v : $|\tau_k - \lambda| < T_v$ and $|\tau_k - L| < T_v$.

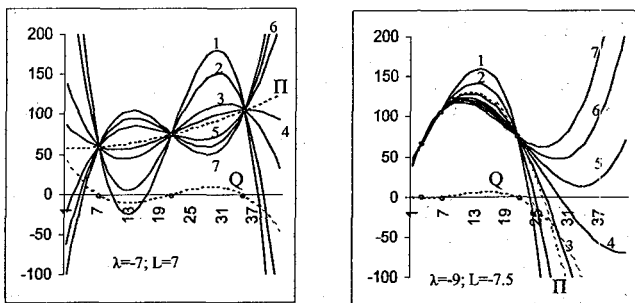


Fig. 3. Changing shapes of cubic curves depending upon chose of $\theta_m, m=1, \dots, 7$.

The stability of the 4-point transforms to a random noise plays an important role for their using in data analysis. Let us consider this property in more detail.

2.3. Stability of DPT to random errors

Transformation (3) is stable to random errors. This property has been used in development of adaptive projective filters for track finding (APF) [13] and other algorithms for function approximation and smoothing [15-17].

The 4-point transform has a number of properties useful for applications. For example, if $f(x)$ is a polynomial of a degree n , then $f^{\circ}(x; \mathfrak{R})$ will be a polynomial of degree $n-2$. The square-law parabola and the straight line are transformed to a constant and the constant is transformed to itself. Using of the 4-point transform to the TPS-model gives us:

$$S^{\circ}(\tau; \mathfrak{R}, \theta) = \Pi^{\circ}(\tau; \mathfrak{R}) + \theta Q^{\circ}(\tau; \lambda, L) = S_0 + \theta \lambda L \tau, \quad (10)$$

i.e. the cubic parabola is transformed to the straight line with parameters $\theta \lambda L$ and S_0 .

For the noise cubic parabola, the observed vector $\tilde{\mathbf{S}}$ looks as a sum of two vectors $\tilde{\mathbf{S}} = \mathbf{S} + \mathbf{E}$, where $\mathbf{S}^T = [S_\lambda, S_L, S_x]$ and $\mathbf{E}^T = [e_\lambda, e_L, e_x]$ is the error vector. The four-point transformation of the noise cubic curve $\tilde{S}(x; \mathfrak{R})$ gives the following result:

$$\tilde{S}^{\circ}(x; \mathfrak{R}) = (\tilde{\mathbf{S}}, \mathbf{P}) = (\mathbf{S}, \mathbf{P}) + (\mathbf{E}, \mathbf{P}) = \tilde{S}_0 + \theta \lambda L \tau + e_x^{\circ},$$

i.e. error e_x is transformed as

$$e_x^{\circ} = (\mathbf{E}, \mathbf{P}) = \varepsilon_x. \quad (11)$$

This error equation shows that the 4-point transformation of $\{\tilde{S}_k\}$ suppresses a random error by a square-law form since e_k is transformed through a denominator of p_{ik} (5). Thus, if errors e_0, e_λ, e_L, e_x of four points on the curve follow the linear-quadratic function, then using error vector $\mathbf{E}_0^T = [e_\lambda - e_0, e_L - e_0, e_x - e_0]$ we obtain

$$(e_k - e_0)^{\circ} = (\mathbf{E}_0, \mathbf{P}_k) = 0. \quad (12)$$

Eq. (12) indicates the stability of transformation to such systematization. This property allows one to apply the procedure of a simple linear regression for smoothing $\{\tilde{S}_k^{\circ}\}$ instead of initial $\{\tilde{S}_k\}$ and then by using the inverse transform (4) to recover the smoothed initial curve. This way gives a number of advantages in comparison with the traditional approach to the curve fitting using the cubic model. The plots of the 4-point transformation over a noised cubic curve $\{S_k\}$, $\mu = -23, m = -37, k = 1, 2, \dots, 100$ are shown in Fig. 4.

The relation $e_k^{\circ}/e_k = (S_k^{\circ} - S_k^{\circ}) / (S_k - S_k)$ is demonstrated in the bottom. From the plots we see that this relation is reduced by more than 75% at the half of the interval. The stability of DPT to random errors and properties (10), (12) are very useful in processing scattered data and we shall use the above results for the development of the smoothing algorithm.

For example, in approximation of the curve the fixed points are known and we should calculate only $\hat{\theta}$, n_θ and x_b, x_e . For curve smoothing we can use, first rough estimations of the pivot coordinates for calculation of $\hat{\theta}$, n_θ, x_b, x_e and then find \mathbf{R}_0 , using the obtained values.

If the variance σ_e^2 is gross, then the initial vector $\tilde{\mathbf{R}}_0$ must be chosen carefully. For example, we can correct $\tilde{\mathbf{R}}_0$ by ordinary averaging the pivot ordinates over three neighboring points.

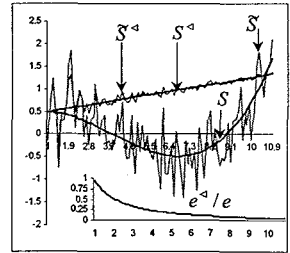


Fig. 4. e°/e for \tilde{S}_k and \tilde{S}_k° .

The main difficulty arises in finding the segment of the curve which adequately fits the shape of the TPS-model. A discrepancy between such shapes produces a deviation of transformed points from a straight line. This discrepancy increases the error in estimation of $\hat{\theta}$ and is used as a test for the interval boundary.

An additional point to emphasize is that the influence of errors in $\tilde{\mathbf{R}}_0$ on the precision of smoothing (approximation) and the length of the interval $[x_b, x_e]$ can be adjusted by selection of parameters λ and L . The actual form of the cubic model $S(x; \hat{\theta})$ depends essentially on such parameters as h, T_f, T_v, σ_e^2 and on complexity of $f(x)$ as well.

3. The recursive cubic smoothing

This section deals with the iterative procedure for finding $\hat{\theta}$. The procedure is based on the TPS-model. It uses 4-point transforms and the first order recursive least squares method (RLSM). The estimations of $\hat{\theta}$ for S_j in (1)-(2) are found in two stages: first, the estimate $\hat{\theta}$ and n_θ are derived. Secondly, the fixed parameters $\tilde{\mathbf{R}}_0$ are corrected by means of the standard LSM-procedure using $\hat{\theta}$ and n_θ . A simple cubic smoother (LOCUS) is constructed for curve smoothing (approximation).

3.1. The iterative procedure for calculation of $\hat{\theta}$

Let the curve be represented as sequence observations in a discrete form and assigned with a step of grid h , i.e. $\tilde{f}_i = f(x_i) + e_i$, $x_i = a + ih$, $x_i \in [a, b]$. For definiteness, we suppose that $e_i \sim N(0, \sigma_e^2)$. If $\sigma_e^2 = 0$, then a set of coordinates of the curve is defined analytically $\tilde{f}_i \equiv f(x_i)$, $i = 0, 1, 2, \dots, N$, $N \gg 4$ and we are dealing with approximation.

Modern experiments are frequently dealt with data flows that form a temporary sequence and there is a need to estimate parameters at any moment of time using the information accumulated up to this moment. In this case a recurrence calculation of the least squares estimations is used.

When n is known, the estimation $\hat{\theta}$ in (7) can be obtained from a minimum condition of a sum of squares of the deviations transformed by a direct DPT:

$$\sum_{k=1}^n (\varepsilon_k^a)^2 \rightarrow \min_{\hat{\theta}}.$$

To derive a recurrence formula for computation $\hat{\theta}_n$ through $\hat{\theta}_{n-1}$, we use Eq. (9). Calculating $\hat{\theta}_{n-1}$ at first, for $n-1$ points and then $\hat{\theta}_n$ for n , we obtain the following relation:

$$\hat{\theta}_n = \hat{\theta}_{n-1} + \tau_n (\lambda L \sum_{k=1}^n \tau_k^2)^{-1} [\tilde{\phi}_n^a - \hat{\theta}_{n-1} \lambda L \tau_n].$$

Let us denote the term $\tau_n (\lambda L \sum_{k=1}^n \tau_k^2)^{-1}$ by $\gamma_n \equiv \gamma(\tau_n; \lambda, L)$. The expression in the square brackets is equal to the 4-point transformation of deviations ε at the point τ_n :

$$\varepsilon_n^a = [\tilde{\phi}_n - S_n(\lambda, L; \hat{\theta})]^a.$$

Hence, at $\tau_n = nh$, $\lambda = \mu h$, $L = mh$ and in view of the equality

$$\sum_{k=1}^n k^2 = \frac{n(n+1)(2n+1)}{6}$$

we obtain

$$\hat{\theta}_n = \hat{\theta}_{n-1} + \gamma_n [\tilde{f}_n^{\text{st}} h^{-3} - \hat{\theta}_{n-1} \mu m n], \quad \hat{\theta}_0 = 0, \quad n = 1, 2, \dots, \quad (13)$$

where

$$\gamma_n = \frac{6}{\mu m (n+1)(2n+1)}. \quad (14)$$

The value $\hat{\theta}_0$ is taken to be equal to zero. An inequality $|r_n| \geq T_f$ is used as the criterion of ending the iteration (13). The residual r_n is calculated in the form

$$r_n = \tilde{f}_n - (\tilde{\mathbf{R}}_0, \mathbf{D}_n) - \hat{\theta}_n \mathcal{Q}_n = \tilde{\phi}_n - (\hat{\mathbf{V}}_n, \mathbf{W}_n), \quad (15)$$

where $\hat{\mathbf{V}}_n^T = [\hat{\theta}_\lambda, \hat{\theta}_L, \hat{\theta}_n]$ is the vector of the parameters and $\mathbf{W}_n^T = [d_{1n}, d_{2n}, \mathcal{Q}_n]$ is the weight vector. Parameter T_f denotes an accuracy threshold.

At the moment the iterative process is finished, the value $n_\theta \equiv n$ defines the number of points (samples), which has been used for obtaining the estimate $\hat{\theta} \equiv \hat{\theta}_n$. Afterward end-points or knots of the local spline are defined as $x_b = x_0$ and $x_e = x_0 + n_\theta h$.

Notice that Eq. (13) is well known in the stochastic approximation theory as the Robbins-Monroe (RM) procedure [10], which is related to a general class of the recursive algorithms used for the solving of equations of the following view

$$g(\Omega) = E\{G(y, \Omega)\} = 0,$$

where G is a known function of the input signal y , Ω - a vector of unknown parameters and $E\{\cdot\}$ is a mean value symbol. Such algorithms are used, for example, to find roots or extremum searching of a regression function. The standard RM-procedure for correction of Ω on the base of the sequence observations y_k is

$$\hat{\Omega}_k = \hat{\Omega}_{k-1} + \gamma_k G[y_k, \hat{\Omega}_{k-1}], \quad k = 1, 2, \dots, \quad (16)$$

where γ_k is a special picked sequence that should satisfy the following conditions:

$$\lim_{k \rightarrow \infty} \gamma_k = 0, \quad \sum_{k=1}^{\infty} \gamma_k = \infty \quad \text{and} \quad \sum_{k=1}^{\infty} \gamma_k^2 < \infty. \quad (17)$$

The second condition guarantees a sufficient number of the correction steps that allows one to approach close the required solution, whereas the third condition guarantees a finiteness of the variance of the noise accumulated. \hat{G} is a limited and unbiased estimation of G : $E\{\hat{G}\} = G$, i.e. G is a regression function for stochastic process \tilde{G} . In the fulfillment of conditions (17) the procedure (16) converges in meansquare sense [10], i.e.

$$\lim_{k \rightarrow \infty} E\{(\Omega_k - \Omega_0)^2\} = 0, \quad \text{where } \Omega_0 - \text{the root of equation } G = 0.$$

The stochastic approximation methods are being applied in a diverse set of field, such as engineering, biology, theory of management, training, etc. Though the convergence of the stochastic approximation method is proved strictly mathematically, its practical application does not always satisfy the solving of applied problems as this convergence is shown at $k \rightarrow \infty$. In practical calculations it is necessary to investigate some extreme vicinity for a small number of steps [14]. Therefore, the question of choosing the amplification

factor γ_k determining the speed of adaptation and convergence of the procedure (16) is rather important. As is known, the harmonic sequence $\{\gamma_k = 1/k^q\}$, $1/2 < q \leq 1$, $k = 1, 2, \dots$ satisfying the conditions (17) finds its wide practical application.

Turning back to the recurrence formula (13), we see that the expression in the square brackets corresponds to the function $G[\gamma_k, \hat{\Omega}_{k-1}]$ from (16), i.e.

$$G[\tilde{\varphi}_n^q, \hat{\theta}_{n-1}] = \tilde{\varphi}_n^q h^{-3} - \hat{\theta}_{n-1} \mu m n.$$

In regards to the sequence $\{\gamma_n\}$ (14), only the first and the third conditions from (17) are strictly fulfilled for it, i.e.

$$\lim_{n \rightarrow \infty} \gamma_n = 0 \text{ and } \sum_{n=1}^{\infty} \gamma_n^2 = \frac{12}{\mu^2 m^2} (2\pi^2 - 24 \ln 2 - 3) < \infty.$$

The second condition is not fulfilled because of corresponding series converges, i.e.

$$\frac{6}{\mu m} \sum_{n=1}^{\infty} \frac{1}{(n+1)(2n+1)} = \frac{6}{\mu m} (2 \ln 2 - 1) < \infty.$$

However, the sum of the series achieves the limit since $n \approx 10^9$. That is really enough for an effective practical application of the suggested method. The sequence $\{\gamma_n\}$ (14) tends to zero much faster than a harmonic sequence.

The denominator of (14) is quadratic in n and depends on indices μ and m . This gives us a possibility for accelerating the convergence and suppressing errors more effectively. By suitable choice of μ and m , one can achieve the rapid convergence which can exceed the cubic convergence (Fig. 5).

Rewriting Eq. (13) in terms of the Eq. (3), we obtain

$$\begin{aligned} \theta_n &= \theta_{n-1} + \gamma_n [(\mathbf{Y}_n, \mathbf{P}_n) h^{-3} - \theta_{n-1} \mu m n] = \\ &= \theta_{n-1} + \gamma_n [(\mathbf{Y}_n, \mathbf{P}_n) h^{-3} - \theta_{n-1} \mu m n] + \gamma_n [(\mathbf{E}_n, \mathbf{P}_n) h^{-3}], \quad n = 1, 2, \dots, \end{aligned} \quad (18)$$

where $\mathbf{E}_n^T = [e_2 - e_0, e_L - e_0, e_n - e_0]$ is the vector of errors for the variable point $\tilde{\varphi}_n$.

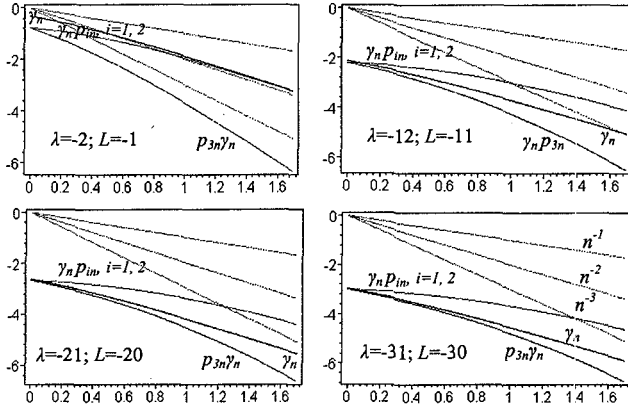


Fig. 5. $\text{Lg}[\gamma_n(\lambda, L)]$ and $\text{lg}|\gamma_n(\lambda, L) P_{in}(\lambda, L)|$ (plots of $\text{lg } n^{-i}$ are shown for comparison)

Hence it follows that the vector of errors in Eq. (13) is transformed through denominators of terms $\gamma_n(\lambda, L) P_{in}(\lambda, L)$, $i = 1, 2, 3$. Graphs of these terms are presented in Fig. 5 for various λ and L in the logarithmic scale in both axes. As we see, the errors in fixed

points $e_\lambda - e_0$ and $e_L - e_0$ can be effectively suppressed by choice of λ and L values. By this is meant that we can calculate the estimate $\hat{\theta}$ in spite of the noise in the pivot ordinates. Mention must be made that $e_\lambda - e_0$ and $e_L - e_0$ are unchanged for fixed $\tilde{\mathbf{R}}_0$.

Taking into account Eqs. (5) and (14), the choice of values of λ and L must satisfy the following two conditions (stability conditions):

- a) values of λ and L must be negative numbers ($\lambda < 0$, $L < 0$);
- b) the greater absolute values of these parameters, the better error suppressing.

The item a) means that the pole points should lay always to the left of a basic point x_0 , whereas the item b) means that these points should lay closer to each other, but as far as possible further from the basic point.

3.2. Correction of the pivot points

As was mentioned above, an ordinary averaging on three ordinates near the pivot points can reduce the influence of a gross error in the fixed parameters. When we use approximation, the fixed parameters are known and the correction procedure is not required.

After shifting the origin in the point (x_0, \tilde{f}_0) , the fixed parameters change as $\tilde{\theta}_\lambda = \tilde{R}_\lambda - \tilde{R}_0$, $\tilde{\theta}_L = \tilde{R}_L - \tilde{R}_0$, and the vector $\tilde{\mathbf{R}}_0$ in the equation of the reference parabola goes in the vector $\tilde{\mathbf{C}}^T = [\tilde{\theta}_\lambda, \tilde{\theta}_L]$.

To correct $\tilde{\theta}_\lambda$ and $\tilde{\theta}_L$ we use $\hat{\theta}$, n_θ and the standard LSM for minimization of the following functional

$$\chi^2 = \sum_{k=1}^{n_\theta} (\hat{\phi}_k - U_k)^2 \rightarrow \min_{\theta_\lambda, \theta_L},$$

where $U_k = \theta_\lambda d_{1k} + \theta_L d_{2k}$, $\hat{\phi}_k = \tilde{\phi}_k - \hat{\theta} Q_k$ and $Q_k = h^3 Q(k; \mu, m)$.

The LSM estimate of $\tilde{\mathbf{C}}^T = [\hat{\theta}_\lambda, \hat{\theta}_L]$ is written as

$$\tilde{\mathbf{C}}^T = (\mathbf{A}^T \mathbf{A})^{-1} \tilde{\mathbf{B}}, \quad (19)$$

where $\mathbf{A}^T \mathbf{A}$ - a nonsingular symmetric matrix of 2×2 , with $\sum d_{1k}^2$, $\sum d_{2k}^2$ on the diagonal, $\sum d_{1k} d_{2k}$ - off-diagonal matrix element, and the vector of the right-hand side is equal to $\tilde{\mathbf{B}}^T = [\sum \hat{\phi}_k d_{1k}, \sum \hat{\phi}_k d_{2k}]$.

Afterward, we obtain the correction of the constant term $\tilde{R}_0 \equiv \tilde{\theta}_{x_0}$ using $\hat{\theta}_\lambda$, $\hat{\theta}_L$, $\hat{\theta}$ and n_θ by the following form:

$$\theta_{x_0} = \frac{1}{n_\theta} \sum_{k=1}^{n_\theta} (\tilde{f}_k - \tilde{U}_k - \theta_\lambda Q_k) d_{3k}^{-1}. \quad (20)$$

Thus, we have obtained the estimates for all four parameters of the TPS model. We can use these results for the development of an algorithm of solving the task (1)-(2).

3.3. Algorithm LOCUS

The above-described DPT-approach to the curve approximation and the smoothing is a good tool for construction of the local cubic smoother - LOCUS. The algorithm LOCUS is designed using equations (7), (13-15), (19) and (20) in following steps:

Start: $\theta_0 = 0$;

$$\hat{\theta} : \tilde{\phi}_n^a = (\tilde{\mathbf{Y}}_n, \mathbf{P}_n); \gamma_n = 6 / [\mu m(n+1)(2n+1)];$$

$$\hat{\theta}_n = \hat{\theta}_{n-1} + \gamma_n [\tilde{\phi}_n^a h^{-3} - \hat{\theta}_{n-1} \mu m n]; \quad (21)$$

$$r_n = \tilde{\phi}_n - (\hat{\mathbf{V}}_n, \mathbf{W}_n), n = 1, 2, \dots;$$

$$\hat{\theta} = \hat{\theta}_n; n_\theta = n; x_b, x_c;$$

$$\hat{\mathbf{R}}_0 : \hat{\mathbf{C}}^T = (\mathbf{A}^T \mathbf{A})^{-1} \mathbf{B}; \hat{\theta}_{x_0}.$$

The values $\gamma_n, \mu m n, d_{1n}^2, d_{2n}^2, d_{1n} d_{2n}, Q_n$, and the vectors $\mathbf{P}_n, \mathbf{D}_n, n = 1, 2, \dots, n_{\max}$ are saved as a look-up table (LUT) for appropriate window.

As seen from (21), the algorithm LOCUS is carried out in two stages. At the first stage the values $\hat{\theta}$ and n_θ are found using DPT, RLSM and the fixed parameters $\tilde{\mathbf{R}}_0$. At the second stage the values $\hat{\theta}$ and n_θ are used for deriving $\hat{\mathbf{R}}_0$. The structure of the LOCUS algorithm (21) is shown in Fig. 6.

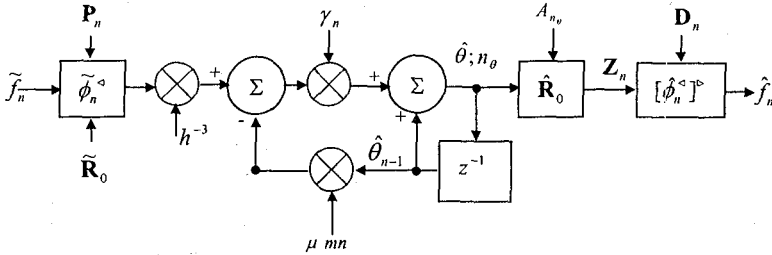


Fig. 6. The flow chart of LOCUS

To restore $\hat{f}(x), x \in [x_b, x_c]$ by (7), four weight functions and nine parameters $x_0, \lambda, L, \theta, \theta_\lambda, \theta_L, \theta_{x_0}, x_b, x_c$ are used. This number can be reduced using the relations between coordinates of pivot points and coefficients $\theta_2, \theta_1, \theta_0$ [13] in the standard cubic form $C(x) = \theta_3 x^3 + \theta_2 x^2 + \theta_1 x + \theta_0$ as follows

$$\theta_2 = (\lambda R_L - L R_\lambda) / (\lambda L H), \theta_1 = (\lambda^2 R_L - L^2 R_\lambda) / (\lambda L H), \theta_0 = R_0.$$

Then recovered by LOCUS estimations $\theta_3 \equiv \hat{\theta}, \hat{\mathbf{R}}_0, x_b, x_c$ and parameters of the weight functions λ and L can be converted into the set of output parameters

$$\hat{\Theta} = \{\hat{\theta}_3, \hat{\theta}_2, \hat{\theta}_1, \hat{\theta}_0\},$$

completely determining the j -th local cubic spline

$$S_j(x; \hat{\Theta}) = \hat{\theta}_3 x^3 + \hat{\theta}_2 x^2 + \hat{\theta}_1 x + \hat{\theta}_0, x \in [x_b, x_c], j = 1, 2, \dots, M.$$

Remark 1. As noted above, the parameters λ and L must satisfy the stability conditions a) and b) for effective suppressing of errors in the pivot ordinates (see Eq. (14) and Fig. 5). This involves difficulties on the starting phase of the smoothing because a few starting points at an interval (λ, θ) are not processed. To avoid this difficulties, we shall calculate the estimate $\hat{\theta}$ by using a new approach - a passage to computation on parameters.

4. A passage to computation on the parameters

The parameters λ and L in the TPS-model (7) are fixed values and τ is a variable value. To underline this, we rewrite Eq. (7) in the following form:

$$S(\tau; \Theta) = S_3(\tau; \mathfrak{R}) = (\mathbf{R}_0^*, \mathbf{D}(\tau; \lambda^*, L^*)) + \theta Q(\tau; \lambda^*, L^*), \quad (7a)$$

where the asterisk indicates the parameters, which remain fixed in calculations.

For this case the regression model is written as follows:

$$S(\tau; \Theta) = \Pi(\tau; \mathbf{R}_0^*) + \theta Q(\tau; \lambda^*, L^*) + e(\tau), \quad (22)$$

$$\lambda < 0, L < 0, \tau > 0, \lambda \neq L \neq 0, \tau = 1, 2, 3, \dots,$$

where $\{e(\tau)\}$ is the white noise process.

The amplification coefficient γ_n depends on τ_n , λ^* and L^* . As indicated above, the choice of λ^* and L^* must satisfy the stability conditions (Fig. 5), i.e. the points positioned between the right pole and the basic point $\tau = 0$ are not used in processing on a starting phase. To remedy this, we use (in view of *continuity of the curve parametrization* [9]) a passage from variable τ towards computation on the parameters λ and L and rewrite Eq. (22) as

$$S(\tau^*; \lambda, L; \mathbf{R}_0^+) = \Pi(\tau^*; \mathbf{R}_0^+) + \theta Q(\tau^*; \lambda, L) + e(\tau^*), \quad (23)$$

where τ^* is fixed and λ, L are variables. Vector \mathbf{R}_0^+ keeps one variable $R_{0\tau}$ and two fixed points $R_{\lambda_0}^+, R_{L_0}^+$, i.e. $\mathbf{R}_0^+ = [R_{\lambda_0}^+, R_{L_0}^+, R_{0\tau}]^T$. This implies that the basic point in the quadruple becomes a moving point. Two curve points $R_{\lambda_0}^+, R_{L_0}^+$ are fixed for the starting values λ_0 and L_0 and the other two points $R_{0\tau} \equiv y(0_\tau)$, $R_\tau \equiv y(\tau)$ are changed with respect to moving the origin 0_τ along the axis τ with a predetermined step of grid h (Fig. 7b). In moving coordinates distances from origin to λ_0 and L_0 are variables and the distance from the origin 0_τ to τ^* remains invariable. If points λ_0 and L_0 are situated from the left of 0_τ , then values λ_n and L_n are increment at $-h$, when the origin moves to the right, i.e. $\lambda_n = \lambda_{n-1} - h$, $L_n = L_{n-1} - h$, $n = 1, 2, 3, \dots$. The weights $d_i(\tau^*; \lambda, L)$, ($\tau^* = h$, $i = 1, 2, 3$) become the homographic functions of λ, L and the cubic parabola Q turns into a square-low function of λ, L :

$$w_{1n} \equiv d_1(h; \lambda_n, L_n) = \frac{-h(h - L_n)}{\lambda_n(L_n - \lambda_n)}, \quad w_{2n} \equiv d_2(h; \lambda_n, L_n) = \frac{h(h - \lambda_n)}{L_n(L_n - \lambda_n)},$$

$$w_{3n} \equiv d_3(h; \lambda_n, L_n) = \frac{(h - \lambda_n)(h - L_n)}{\lambda_n L_n}, \quad Q_n \equiv Q(h; \lambda_n, L_n) = h(h - \lambda_n)(h - L_n), \quad (24)$$

where $\lambda_n = \lambda_0 - nh$, $L_n = L_0 - nh$, and $\sum_{i=1}^3 w_{in} = 1$.

Such a trick allows one to simplify the estimation of the parameter θ in (23). In this situation the errors e_{λ_0} , e_{L_0} are suppressed yet on the starting phase.

Let us consider this case in detail. For the quadruple $\{\lambda_n, L_n, 0_n, h\}$, the TPS-model is written as follows

$$S_n = R_{\lambda_0}^* w_{1n} + R_{L_0}^* w_{2n} + R_{0_n} w_{3n} + \theta Q_n + e_n, \quad n = 1, 2, 3, \dots,$$

where $t^* = t_{0_n} + h$, $\lambda_n = \lambda_0 - nh$ and $L_n = L_0 - nh$ (0_n is the n -th origin shift).

When the origin moves to the right per h , two number consequences appear:
 $\lambda_n = (\mu_0 - n)h = \mu_n h$ and $L_n = (m_0 - n)h = m_n h$, $n = 1, 2, 3, \dots$, where μ_0, m_0 - the indices for λ_0, L_0 ; ($\lambda_0 < L_0 < 0$). Substituting these expressions into Eqs. (24) gives

$$\begin{aligned} w_{1n} &\equiv w_1(\mu_n, m_n) = \frac{-(1 - m_n)}{\eta_0 \mu_n}, \\ w_{2n} &\equiv w_2(\mu_n, m_n) = \frac{(1 - \mu_n)}{\eta_0 m_n}, \\ w_{3n} &\equiv w_3(\mu_n, m_n) = \frac{(1 - \mu_n)(1 - m_n)}{(\mu_n)(m_n)}, \\ Q_n &\equiv Q_n(\mu_n, m_n) = h^3(1 - \mu_n)(1 - m_n), \end{aligned} \quad (25)$$

where $\eta_0 = m_0 - \mu_0$. Let $\mu_0 = -2$, $m_0 = -1$, $\eta_0 = 1$. Then $\mu_n = \mu_0 - n$, $m_n = m_0 - n$, and the expressions for w_{in} and Q_n are written as

$$w_{1n} = 1, \quad w_{2n} = -\frac{(n+3)}{(n+1)}, \quad w_{3n} = \frac{(n+3)}{(n+1)}, \quad Q_n = h^3(n+3)(n+2), \quad n = 1, 2, 3, \dots \quad (26)$$

It is interesting to note that in the passage to computing on the parameters, the cubic parabola $Q_n = Q(\tau_n)$ is turned to quadratic parabola $Q_n = Q(n)$ for fixed h . As it follows from (26), $\lim_{n \rightarrow \infty} |w_{in}| \rightarrow 1$, $i = 2, 3$ (Fig. 7a).

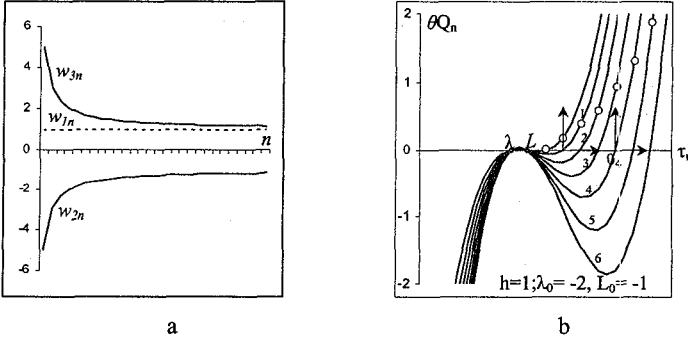


Fig. 7. Plots of w_{in} (a) and $Q_n(\tau)$ for the moving coordinates to the right (b) (the values of $Q_n(n) = h^3(n+3)(n+2)$ are signed by circles).

Let $\{t_k, \bar{y}_k\}_{k=1}^K$, $K \gg 4$, $\bar{y}_k = y_k + e_k$, $t_k = t_{k-1} + \Delta t$ and $e_k \sim N(0, \sigma^2)$. Let us take, for example, three points $t_{\lambda_0} < t_{L_0} < t_0$ and fix two samples $\bar{y}_{t-t_{\lambda_0}} \equiv \bar{R}_{\lambda_0}^*$ and $\bar{y}_{t-t_{L_0}} \equiv \bar{R}_{L_0}^*$. Other two points in the quadruple $\{\lambda_n, L_n, 0_n, h\}$ $\bar{y}_{t-t_0} \equiv \bar{R}_{0_n}$ and \bar{y}_t are variables with respect to the starting origin, but they are fixed relative to 0_n at $t_{0_n} = 0$ and $t^* = t_{0_n} + h = h$. In this case, in order to obtain recursive formula for calculation of the estimate θ_n , we shall use Eq. (23) and a functional

$$\Phi(\theta) = \sum_{k=1}^n [\bar{y}_k - \bar{\Pi}_k(\bar{R}_k^*) - \theta Q_k]^2.$$

Using the necessary condition of the minimum $\frac{\partial \Phi}{\partial \theta} = 0$, first for $n-1$ and then for n points, we obtain the following recursion:

$$\theta_n = \theta_{n-1} + \gamma_n [\bar{y}_n - \bar{\Pi}_n - \theta_{n-1} Q_n], \quad \theta_0 = 0, \quad n = 1, 2, 3, \dots, \quad (27)$$

where

$$\gamma_n = \frac{Q_n}{\sum_{k=1}^n Q_k^2}.$$

Let us rewrite the Eq. (27) in the following form:

$$\hat{\theta}_n = \hat{\theta}_{n-1} + \gamma_n [\bar{y}_n - (\hat{\mathbf{R}}_{0n}^+ \mathbf{W}_n) - \hat{\theta}_{n-1} Q_n], \quad \theta_0 = 0, \quad n = 1, 2, 3, \dots \quad (28)$$

where $\mathbf{W}_n = [w_{1n}, w_{2n}, w_{3n}]^T$ and $\hat{\mathbf{R}}_{0n}^+ = [\bar{y}_{\lambda_0}, \bar{y}_{L_0}, \bar{y}_{0n}]^T$.

If we substitute Q_n from Eqs. (26), then we derive the expression for γ_n :

$$\gamma_n = \frac{(n+2)(n+3)}{h^3 \sum_{k=1}^n (k+2)^2 (k+3)^2} \quad \text{or} \quad (29)$$

$$\gamma_n = \frac{(n+2)(n+3)h^{-3}}{\frac{1}{5}(n+1)^5 + 2(n+1)^4 + \frac{23}{3}(n+1)^3 + 14(n+1)^2 + \frac{182}{15}n - \frac{358}{15}}.$$

In this case, the errors in Eq. (28) are transformed as follows

$$\mathcal{E}_n = \gamma_n e_n - \gamma_n (\mathbf{E}_{0n}^+, \mathbf{W}_n), \quad n = 1, 2, 3, \dots, \quad (30)$$

where e_n is an error of \bar{y}_n , and $\mathbf{E}_{0n}^+ = [e_{\lambda_0}, e_{L_0}, e_{0n}]^T$ is the error vector of the pivot points. From Eq. (30) it follows that e_{λ_0} and e_{L_0} are multiplied by $\gamma_n w_{1n}$ and $\gamma_n w_{2n}$, while $e_{0n} \equiv e_{n-1}$ and e_n are multiplied by $\gamma_n w_{3n}$ and γ_n , respectively.

If we use Eq. (22) with variable τ and fixed λ^* and L^* (a general case), then Eq. (27) gives the amplification factor in the following view

$$\gamma_n = Q(\tau_n; \lambda^*, L^*) \left[\sum_{k=1}^n Q^2(\tau_k; \lambda^*, L^*) \right]^{-1}.$$

In this case e_{λ_0} and e_{L_0} are transformed by the factors $d_{in}(\tau) \gamma_n(\tau)$. Plots $\gamma_n(\tau)$ and $\gamma_n(\tau) d_{3n}(\tau)$ are shown in Fig. 8b. So, the absolute values of all errors in computing $\hat{\theta}_n$ (Eqs. 28, 29) is suppressed nearly as $1/n^3$, for $h=1$ and $\lambda=-2, L=-1$ (Fig. 8a). We see, that $\gamma_n w_{in} \sim \gamma_n(1; \lambda_n, L_n)$, $i=1, 2, 3$, while $\gamma_n(\tau) d_{3n}(\tau)$ is much worse in comparison with $\gamma_n w_{in}$ and $\gamma_n(\tau)$ (Fig. 8). It must be underlined that at a starting phase of the smoothing the plots of γ_n and $\gamma_n w_{in}$ are located below of the plot $1/n^3$ (for the first five points).

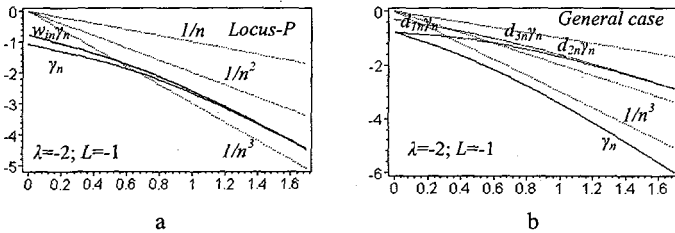


Fig. 8. $\lg \gamma_n$, $\lg |\gamma_n w_{3n}|$ (a) and $\lg \gamma_n(\tau)$, $\lg |\gamma_n(\tau) d_{3n}(\tau)|$ (b).

So, using Eqs. (23) - (30), we can design the algorithm LOCUS-P for estimating the parameter θ , using the first two points $(\bar{y}_{\lambda_0}, \bar{y}_{L_0})$ of the sample as the fixed parameters of the model.

The passage from the variable τ to the parameters λ and L allows one to transform the initial cubic model (22) into a more simple model (23), to increase the degree of the error suppressing in the fixed points at the starting phase of the curve smoothing. This approach allows one to achieve a high stability of the smoothing to random errors and to simplify computations. This features of the smoother are very useful for data analysis including a real-time mode. An empirical study of the algorithm is conducted by using two data set-ups.

The first example is related to the set of scattered equidistant points of the cubic curve (31) and the second one contain the equidistant points scattered around of an ellipse arch (32), $e(x) \sim N(0, \sigma^2)$ (for distinctness).

$$\tilde{f}(x) = 0.5x^3 - 4.2x^2 + 6.715x - 0.63 + e(x), \quad (31)$$

$$\tilde{f}(x) = -5 + \sqrt{169 - 10(x - 3.5)^2} + e(x), \quad x \in [0, 7.5]. \quad (32)$$

MAPLE V procedures *randomize(kern)* and *stats[random,normald[0,sig]](1)* were used for producing the samples $\{\tilde{f}_k = f_k + e_k, k = 1, \dots, K\}$.

Computations of the estimates $\hat{\theta}_n$, R_λ , R_L and R_0 have been derived for various values σ_e . The quality of estimates \hat{f} has been assessed by relative error r_e :

$$r_e = \sqrt{\sum_{i=1}^n (\tilde{f}_i - \hat{f}_i)^2} / \sqrt{\sum_{i=1}^n \tilde{f}_i^2}.$$

The outcomes of these calculations for cubic curve (31) and samples $\{x_k, \tilde{f}_k\}$, $h = 0.1$, $k = 1, \dots, 75$ are shown in Table 1 and Figs. 9. Figures 10a, 10b and 11a, 11b show plots of input and output related to both curves (31), (32) for some of *kern* and σ_e .

Table 1.

σ_e	$\hat{\theta}$	R_λ	R_L	R_0	r_e
0.00	0.500000	0.000000	19.08000	-7.95600	0.000000
0.01	0.491480	0.117536	18.92289	-7.91611	0.010714
0.10	0.494333	0.076368	19.00154	-7.92381	0.015651
0.50	0.507013	-0.10656	19.35109	-7.95807	0.075236
0.75	0.514937	-0.22010	19.56956	-7.97948	0.113964
1.00	0.522862	-0.33531	19.78804	-8.00089	0.152407
2.00	0.554560	-0.79273	20.66192	-8.08654	0.299617
3.00	0.586259	-1.25015	21.53580	-8.17218	0.430996
4.00	0.617958	-1.70757	22.40968	-8.25782	0.542981
5.00	0.649656	-2.16499	23.28356	-8.34347	0.635430
6.00	0.681355	-2.62241	24.15745	-8.42911	0.710272
7.00	0.713054	-3.07983	25.03133	-8.51448	0.770280
8.00	0.744752	-3.53725	25.90521	-8.60040	0.818272
9.00	0.776450	-3.99467	26.77910	-8.68604	0.856741
10.0	0.808150	-4.45209	27.65298	-8.77169	0.887730

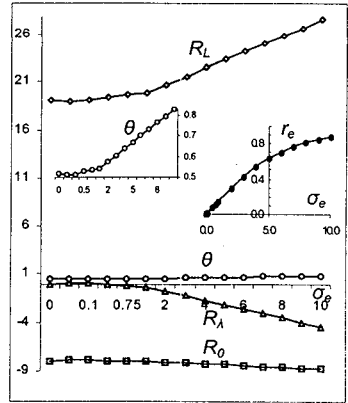


Fig. 9. Estimates of the TPS-parameters for various σ_e .

The plots on the right of Figs. 10, 11 are shown an effect of the error suppressing in fixed and variable actual points. Fig.10b presents a fluctuation of errors \mathcal{E}_n transformed by Eq. (30), which correlate with corrections of $\Delta\hat{\theta}_n$ in the iteration process of computation of $\hat{\theta}_n$ by Eqs. (28), (29).

Input samples are labeled as circles. The estimate $\hat{f}(x)$ is presented by the bold plot, the true function $f(x)$ by the thin plot. Errors distribution or residuals $\tilde{f}_k - \hat{f}(x_k)$ are shown in both, as histogramms and as diagram on the axes $(\tilde{f}_k, \hat{f}(x_k))$. A dynamics

of the errors suppressing and adaptation over the parameter θ are shown, too. We see that the output results are confirmed by real estimates of the curves and the high stability of LOCUS-P to random errors.

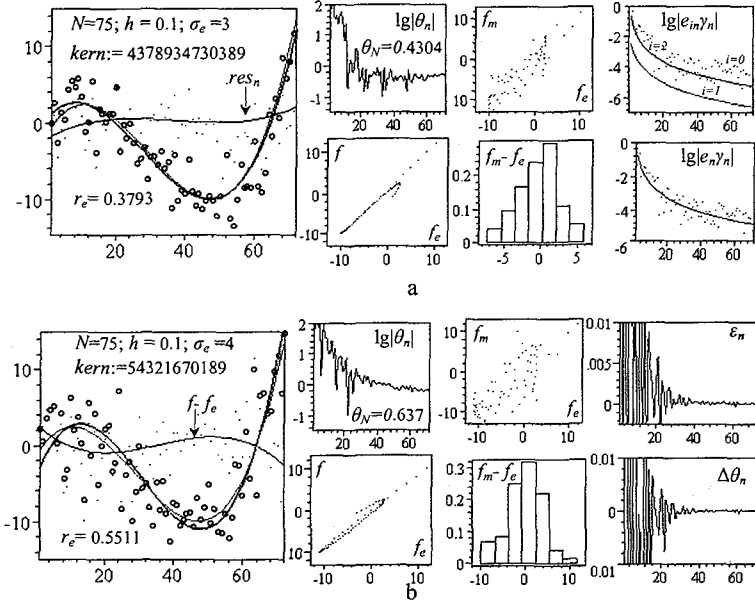


Fig. 10. The smoothing of the cubic curves using the LOCUS-P.

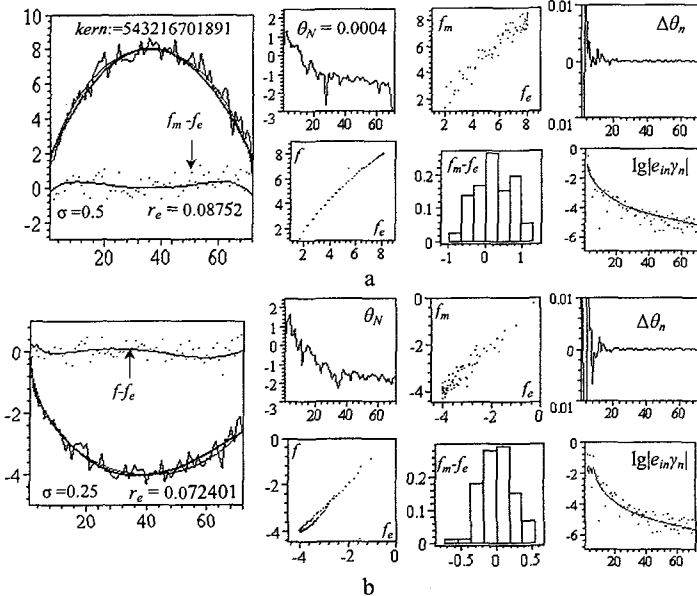


Fig. 11. The smoothing of arches of the ellips and the circle using the LOCUS-P.

Figure 11 shows similar plots related to the arch of ellipse (32) for $\sigma_e=0.5; 0.25$. One can see that the LOCUS-P fits the noise ellipse arch using only one cubic segment. Section 5 considers examples of applying the LOCUS to fitting curves by cubic segments in accordance with the task (1)-(2).

5. Examples

As examples, we shall consider the use of LOCUS for smoothing (approximation) of the arbitrary curve presented by the gross sample size (~ 1000 equidistant points). LOCUS has restored an irregular shape of the curve the seven local cubic segments (Fig. 12). The observed sample (a) and the quality of smoothing (a, c, e, f, g) are shown by plots of the input, the restored curve $\hat{f}(x)$, residuals and deviation of $\hat{f}(x)$ from the true curve. The plot (d) is the number of points included in S_j ($N_j = n_{\theta_j}$). The example of 4-point transformations ($\tilde{\varphi}^a$) for each cubic segment and their smoothing (S_j^a) is shown in window (b).

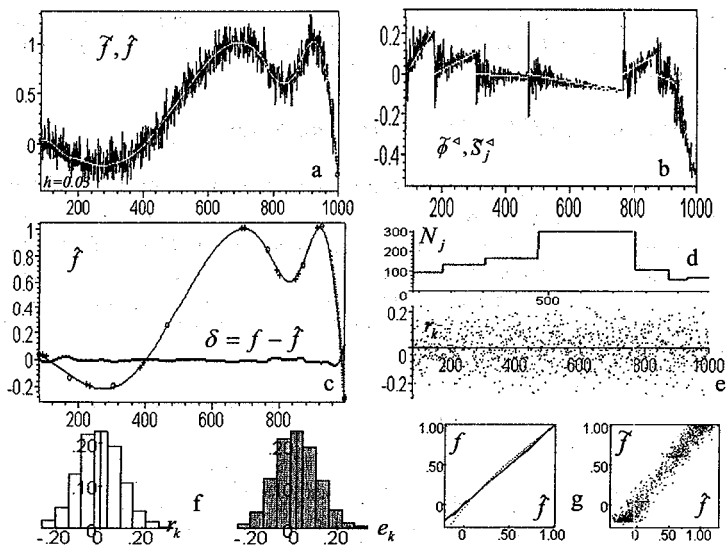


Fig. 12. The example of the curve smoothing by the LOCUS

Input parameters: $K = 867$, $h = 0.03$, $\sigma_e = 0.08$, $T_f = 3\sigma_e$,

Output: $\max |f - \hat{f}| = 0.118$, $K_{inp}/K_{out} = 18$, $r_e = 0.125$

Fig. 13a shows the results of processing the new "observations" (sample size ~ 250), that has been obtained for the above curve. The approximation of the test curve we see in Fig 13b. The number of cubic segments increases because of a greater accuracy.

The process of adaptation of each cubic segment and the plots of amplification factors ($\lg \gamma_{nj}$) are presented in Fig. 13c.

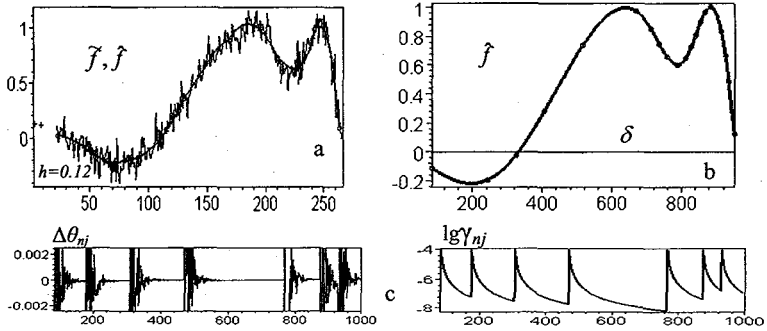


Fig. 13. The example of the curve smoothing and approximation by the LOCUS

Mention must be made that the LOCUS uses three fixed points situated outside the first segment on the left. As remarked above, this difficulty is removed by using the LOCUS-P (see Section 4).

6. Comparison of LOCUS with other smoothers

LOCUS-estimations $\{\hat{f}_{Locus}\}$ have been compared with estimations $\{f\}$ obtained by other non-parametric smoothers, such as *Supersmoother*, *Kernel*, *Loess*, *Spline*, wavelet de-noising [1, 8, 2] and the moving average filter (MAF). To compare LOCUS with other smoothers we use samples, dispersed around of the cubic curves (Figs. 14, 15) and different shapes of curves, such as ellipse arcs, gauss curves. On Fig. 14 we can see, that the LOCUS-estimates have the smaller deviations from the true curve for both MAF and wavelets.

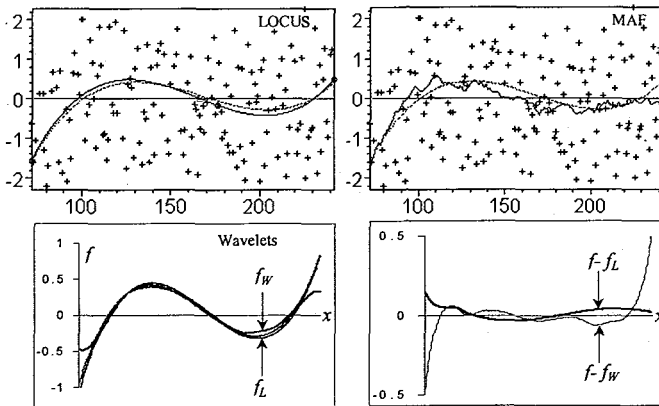


Fig. 14. Comparison of LOCUS-estimates with MAF (15 points in the moving average); (+ - samples, dot lines - the true curve, solid lines - estimates) and wavelet de-noising (*symmlets*). Deviations $f-f_L$ and $f-f_W$ are shown on the right.

Comparison of fitting results for cubic curve using LOCUS-P and *Supersmoother* is presented in Fig. 15. Graphs of deviations $(f - f_{Locus})$ and $(f - f_{Super})$ are shown on the right.

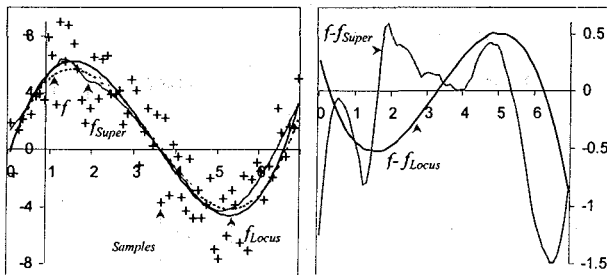


Fig. 15.

The other example relates to fitting of semi-gaussian shaped pulses which used as a signal model in radiation detectors:

$$f = A \exp\left(-\frac{(t-m)^2}{2(s+\alpha(t-m))^2}\right),$$

$$A=1, s=0.8, m=1.325, \alpha=0.225.$$

The amplitude A is proportional to the energy of the detected radiation, m is position of the pulse's extremum and s and α the shape dependent parameters [18].

The sample $\{t_k, \tilde{f}_k\}$, $k=1,2,\dots,75$ has been generated with $kern=543216701819$, $\sigma_e=0.075$ and $h=0.1$ at $0 < t \leq 7.5$ (Fig. 16). Two segments of 17 and 58 points and two sets of the estimates have been found using LOCUS-P:

$$R_{\lambda_1}=0.0039802822, R_{L_1}=0.7828929325, R_{0_1}=0.8302133725, \theta_1=-0.5850435980;$$

$$R_{\lambda_2}=0.8339159463, R_{L_2}=0.09457573661, R_{0_2}=0.00722632226, \theta_2=-0.0085234840.$$

The values R_{e_j} , ($j=1,2$) are derived for $\lambda_j=-L_j=8$, $\lambda_2=-L_2=29$ with respect to midpoints of the segments. The relative error $r_e=0.1481113565$ assess the quality of the smoothing. The dynamics of the smoothing process is shown on the right of Fig. 16.

The same samples have been processed using other smoothing procedures [1,2]. The plot of the output f_L , f_S , the residual histograms r_L , r_S and the deviations $f - f_{Super}$, $f - f_{Locus}$ are shown overhead. We see, that both outcomes are in agreement with the true function f .

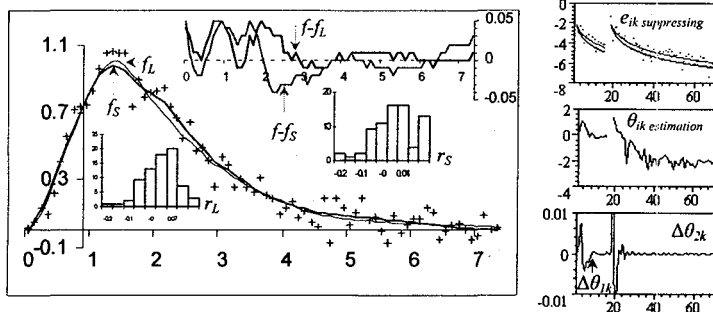


Fig. 16.

The last example (Fig. 17) is related to comparison of the estimates obtained in processing of the noise curve (the arch ellips) (32) with $\sigma_e=3$, using LOCUS-P and four other smoothers: *Kernel*, *Spline*, *Loess* and *Supersmoother*.

The estimate f_{Locus} is expressed by the following cubic curve ($\lambda = -L=36$):

$$f_{Locus} = 2.307530363d_1(x; \lambda) - 0.040161293 d_2(x; \lambda) + 7.98460627d_3(x; \lambda) + 0.01609078556x(x^2 - \lambda^2).$$

The estimates f_{Locus} , f_{Super} and the true function f (dot line) are presented on the left and the plots of f_{Locus} , f_{Kernel} , f_{Loess} and f_{Spline} are shown on the right.

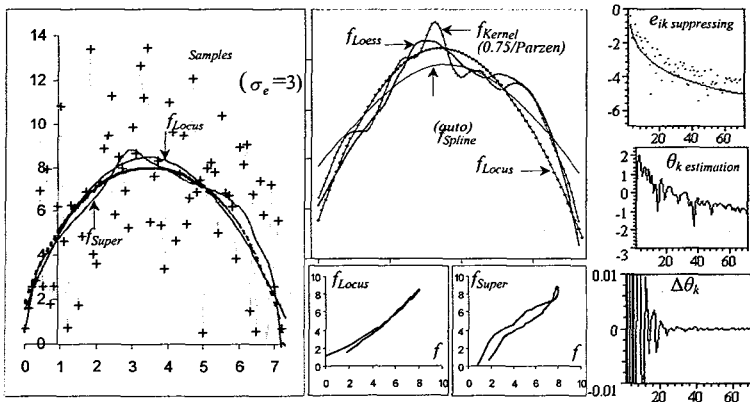


Fig. 17. Comparison of the LOCUS-P estimate with the estimates of other smoothers

Above mentioned examples and the comparison results with other known smoothers demonstrate the performance capabilities of proposed approach and the method for the cubic smoothing in the adaptation mode.

7. Conclusion

The TPS-model and the iterative method for approximation and smoothing of curves by using DPT and the first order recursive least squares method is proposed. The simple local cubic smoother LOCUS is constructed. The algorithm is stable to the additive random noise and has a high adaptation speed. The iterative procedure, type of Robbins-Monroe procedure, is derived to calculate the estimate of free parameter of the TPS-model. The amplification factor is adaptable by parameters μ , m and varies with n as $\gamma_n \propto 1/n^3$.

A concept of a successive definition of parameters is used. It has allowed one to reduce approximately as much as twice a number of operations and it is essential to reduce size of the working memory needed for initial and intermediate data storage.

The performances of the algorithm are investigated by the programmed way. Noise stability and efficiency of the method are confirmed by examples. Comparison of LOCUS output with output of other smoothers is made. The algorithm is very simple in programming, does not require large resources of memory and is focused on its application in digital signal processing, contour processing, track finding and for the numerical solving of many practical problems as well.

The distinctive features of the LOCUS are: a) third order accuracy approximation; b) successive data processing; c) simple computing circuit; d) guaranteed convergence of iterations; e) stability to random errors; f) parametrical adjustment; g) automatic knots definition; h) weight functions are known. These properties provide such characteristics of algorithm, as adaptability (b, d, e, f, g); accuracy (a, e, h); stability (c, e); high speed (c, d); flexibility (a, b, f, h); efficiency (b, c, d, h).

For example, the estimate of speed adaptation LOCUS makes approximately 18 short arithmetic operations per one iterative cycle that twice as less than the number of operations necessary for realization of the recursive least squares algorithm of the third order. It is required approximately 36 operations [3]. The efficiency of the algorithm is estimated by high speed and the memory resources necessary for data storage, programs and working space. In our case these characteristics are quite good, because the calculation of the estimations of the parameters is carried out in a data inflow mode and does not require to storing samples in a complete size. The accuracy of the algorithm is provided by the order of the chosen model, accuracy of weight functions as well as by optimality of the criteria used for calculating the estimations.

Acknowledgement

The author is greatly thankful to Dr. Cs.Török (Technical University of Košice) for help with the wavelet de-noising test and collaboration.

References

- [1] W.Hardle. Applied non-parametric regression, Cambridge Univ. Press, 1990.
- [2] A.Bruce, H.Y.Gao. Wavelet Analysis with S-PLUS, Springer, 1996.
- [3] C.F.N. Cowan and P.M. Grant, eds., Adaptive Filters, Prentice Hall, Englewood Cliffs, 1985.
- [4] R.O. Duda, P.E. Hart. Pattern Classification and Scene Analysis, John Wiley and Sons, 1973.
- [5] E.P. Box and G.M. Jenkins. Time Series Analysis. Forecasting and control, Holden-Day, 1970.
- [6] Lennart Ljung. System Identification: Theory for the User, Prentice Hall, 1987.
- [7] Regler (ed.). Data analysis techniques for high-energy physics experiments, Cambridge University Press, 1990.
- [8] J.H. Friedman. A Variable Span Smoother. Department of Statistics, Stanford University, Tech. Report 5, 1984..
- [9] N.D. Dikoussar. Function parametrization by using 4-point transforms, Comput. Phys. Commun., **99** (1997) 235-254.
- [10] M.T. Wasan. Stochastic Approximation, Cambridge University Press, N.Y., 1969.
- [11] N.D. Dikoussar. A Piecewise Cubic Approximation and the Smoothing of Curves in an Adaptation Mode, Commun. of JINR, P10-99-168, Dubna, 1999 (in Russian).
- [12] G.A.F. Seber. Linear Regression Analysis, John Wiley and Sons, N.Y., 1977.
- [13] N.D. Dikoussar. Adaptive projective filters for track finding, Comput. Phys. Commun., **79** (1994), 39-51.
- [14] A.A. Krasovskij (edit.). Handbook on the Theory of Automatic Control, Nauka, Moscow, 1987 [in Russian].
- [15] Cs. Török and N.D.Dikoussar. Approximation with Discrete Projective Transformation, Comput. and Math. with Appl., **38** (1999) 211-220.
- [16] Cs. Török, 4-Point transforms and approximation, Comput. Phys. Commun. **125** (2000), 154-166.
- [17] N.D. Dikoussar, Cs. Török. On one approach to surface smoothing, Commun. of JINR, P10-99-223, Dubna, 1999 (in Russian).
- [18] J.Basilio Simões, P.C.P.S. Simões and C.M.B.A. Correia. Nuclear Spectroscopy Pulse Height Analysis Based on Digital Signal Processing Techniques, IEEE Transactions on Nuclear Science, **42**, 4 (1995) 700-704.

Received by Publishing Department
on March 21, 2001.

**The Publishing Department
of the Joint Institute for Nuclear Research
offers you to acquire the following books:**

Index	Title
D1,2-98-215	Proceedings of the International Workshop «Relativistic Nuclear Physics: from MeV to TeV». Dubna, 1998 (384 p., in English and Russian)
E2-98-254	Proceedings of the International Workshop «Hadronic Atoms and Positronium in the Standard Model». Dubna, 1998 (260 p., in English)
D9,11-98-273	Proceedings of the 4th International Workshop «Beam Dynamics and Optimization». Dubna, 1997 (162 p., in English and Russian)
E17,19-98-305	Proceedings of the International Workshop on Deuteration of Biological Molecules for Structural and Dynamic Studies. Applications to Neutron Scattering and NMR. Dubna, 1998 (100 p., in English)
E1,2-98-307	Proceedings of the International School-Seminar «Actual Problems of Particle Physics». Gomel, Belarus, 1997 (2 volumes, 304 p. and 220 p., in English)
E2-98-372	Proceedings of the III International Workshop «Classical and Quantum Integrable Systems». Erevan, 1998 (200 p., in English)
E9-99-26	Proceedings of the International Conference on High Energy Accelerators. Dubna, 1998 (432 p., in English)
E2-99-35	Proceedings of the XI International Conference on Problems of Quantum Field Theory. Dubna, 1998 (508 p., in English)
E9-99-92	Proceedings of the XVII International Conference on High Energy Accelerators HEACC'98. Dubna, 1998 (435 p., in English)
E9,18-99-169	Proceedings of the International Symposium SCHEF'99 «Space Charge Effects in Formation of Intense Low Energy Beams». Dubna, 1999 (209 p., in English)
E7,17-99-199	Proceedings of the Research Workshops «Nucleation Theory and Applications». Dubna, 1997, 1998, 1999 (510 p., in English)
E3-99-212	Proceedings of the VII International Seminar on Interaction of Neutrons with Nuclei. Dubna, 1999 (372 p., in English)
D1,2-99-294	Proceedings of the International Workshop «Relativistic Nuclear Physics: from MeVs to TeVs». Stara Lesna, Slovak Republic, 1999 (192 p., in English and Russian)
D2-99-310	Proceedings of the Seminar «Symmetries and Integrable Systems». Dubna, 1999 (317 p., in English and Russian)
D9-2000-69	Proceedings of the III Scientific Seminar in Memory of V.P.Sarantsev. Dubna, 1999 (196 p., in English and Russian)
E15-2000-75	Proceedings of the IV International Workshop «Laser Spectroscopy on Beams of Radioactive Nuclei». Posnan, Poland, 1999 (262 p., in English)

- E2-2000-82 Proceedings of JINR Workshop «Supersymmetries and Quantum Symmetries». Dubna, 1999 (454 p., in English)
- E1,2-2000-166 Proceedings of the XIV International Seminar on High Energy Physics Problems «Relativistic Nuclear Physics and Quantum Chromodynamics». Dubna, 1999 (2 volumes, 256 p. and 320 p., in English)
- E2-2000-172 Proceedings of the International Seminar «Physical Variables in Gauge Theories». Dubna, 1999 (172 p., in English)
- E3-2000-192 Proceedings of the VIII International Seminar on Interaction of Neutrons with Nuclei. Dubna, 2000 (460 p., in English)
- E1,2-2000-208 Proceedings of the International School-Seminar «Actual Problems of Particle Physics». Gomel, Belarus, 1999 (2 volumes, 196 p. and 206 p., in English)
- D2,5-2000-218 Proceedings of the International School «Symmetries and Integrable Systems». Dubna, 1999 (158 p., in English and Russian)
- E2-2000-226 Proceedings of the V International Workshop «Heavy Quark Physics». Dubna, 2000 (154 p., in English)
- E1,2-2000-244 Proceedings of the International Workshop on Very High Multiplicity Physics. Dubna, 2000 (204 p., in English)
- E1,2-2000-248 Proceedings of the Second International Symposium «LHC Physics and Detectors». Dubna, 2000 (3 volumes, in English)
- E1,2-2000-282 Proceedings of the International Workshop «Hot Points in Astrophysics». Dubna, 2000 (406 p., in English)
-

Please apply to the Publishing Department of the Joint Institute for Nuclear Research for extra information. Our address is

Publishing Department
Joint Institute for Nuclear Research
Dubna, Moscow Region
141980 Russia
E-mail: publish@pds.jinr.dubna.su

**SUBJECT CATEGORIES
OF THE JINR PUBLICATIONS**

Index	Subject
1.	High energy experimental physics
2.	High energy theoretical physics
3.	Low energy experimental physics
4.	Low energy theoretical physics
5.	Mathematics
6.	Nuclear spectroscopy and radiochemistry
7.	Heavy ion physics
8.	Cryogenics
9.	Accelerators
10.	Automatization of data processing
11.	Computing mathematics and technique
12.	Chemistry
13.	Experimental techniques and methods
14.	Solid state physics. Liquids
15.	Experimental physics of nuclear reactions at low energies
16.	Health physics. Shieldings
17.	Theory of condensed matter
18.	Applied researches
19.	Biophysics

Дикусар Н.Д.

E10-2001-48

Локально-кубическое сглаживание кривых в режиме адаптации

Предлагается новый подход к решению задачи локальной аппроксимации и сглаживанию кривых. Отношение между точками кривой определяется специальными весовыми функциями сложного отношения четырех точек. Координаты трех опорных точек кривой используются в качестве параметров как для весовых функций, так и для кубической модели сглаживателя (TPS). Создан простой в вычислении и устойчивый к случайным ошибкам кубический сглаживающий фильтр в режиме адаптации (LOCUS). Оценка свободного параметра TPS определяется рекурсивно независимо от фиксированных параметров с эффективным подавлением ошибок в опорных точках и может контролироваться с помощью параметров модели. Эффективность и помехоустойчивость алгоритма подтверждены примерами и сравнением с результатами обработки кривых другими известными непараметрическими сглаживающими фильтрами.

Работа выполнена в Лаборатории информационных технологий ОИЯИ.

Препринт Объединенного института ядерных исследований. Дубна, 2001

Dikoussar N.D.

E10-2001-48

A Local Cubic Smoothing in an Adaptation Mode

A new approach to a local curve approximation and the smoothing is proposed. The relation between curve points is defined using a special cross-ratio weight functions. The coordinates of three curve points are used as parameters for both the weight functions and the three-point cubic model (TPS). A very simple in computing and stable to random errors cubic smoother in an adaptation mode (LOCUS) is constructed. The free parameter of TPS is estimated independently of the fixed parameters by recursion with the effective error suppression and can be controlled by the cross-ratio parameters. Efficiency and the noise stability of the algorithm are confirmed by examples and by comparison with other known non-parametric smoothers.

The investigation has been performed at the Laboratory of Information Technologies, JINR.

Preprint of the Joint Institute for Nuclear Research. Dubna, 2001

Макет Т.Е.Попеко

Подписано в печать 11.04.2001
Формат 60 × 90/16. Офсетная печать. Уч.-изд. листов 2,56
Тираж 300. Заказ 52589. Цена 3 р.

Издательский отдел Объединенного института ядерных исследований
Дубна Московской области